AXIAL BEHAVIOUR OF PRESTRESSED HIGH STRENGTH STEEL TUBULAR MEMBERS

Jie Wang[a], Sheida Afshan[b], Leroy Gardner[c]

a,c Imperial College London, London, UK
b Brunel University London, London, UK

Abstract: The axial behaviour of high strength steel tubular elements with internal prestressing cables, representing the chord members in prestressed trusses, is investigated herein. Experiments on tensile and compressive members were carried out, with the key variables examined being the steel grade (S460 and S690), the initial prestress level and the presence of grout. FE models were developed to replicate the experiments and generate parametric results. The presence of cables was shown to enhance the tensile load-carrying capacity of the members while the application of prestress extended the elastic range. In compression, prestressing was detrimental, and a modified Perry-Robertson design approach was examined.

1. Introduction

Prestressed steel trusses can offer high material efficiency for long span applications such as aircraft hangars, stadia and warehouses [1, 2]. Cable-in-tube systems, whereby the steel cables are housed within hollow structural sections, are one way to achieve these structural forms. The performance of cable-in-tube systems in normal strength steelwork has been studied in [3, 4]. This paper focuses on the behaviour of such systems in high strength steels (HSS).

2. Experiments

2.1 General

To assess the response of cable-in-tube systems with different prestress levels and with addition of grout, a total of 22 specimens were tested under axial loading (12 in tension and 10 in compression). Fig. 1 depicts a typical test specimen. The steel tubes were hot-finished S460 and S690 SHS 50×50×5, which encased Y1860S7 cables. Their material and geometric properties are given in Table 1, where E, f_y and A are the Young's modulus, yield stress and cross-sectional area, respectively. Half of the specimens were grouted. The strength of the grout was derived from cube tests performed on the same day as the member test. The nominal grout strength was 50 N/mm^2.

The key variables of the cable-in-tube specimens were the steel grade (S460 and S690), initial prestress level (No cable, P_{nom}, $0.5P_{opt}$ and P_{opt}) and presence of grout. Fig. 2 gives the labelling system employed throughout the paper. The prestress P_{nom} is a nominal prestress level (around 5 kN) applied to ensure that the cables were taut during grouting and testing. The prestress P_{opt}, as defined in [3], is the optimum initial prestress force that causes the cable and the tube to yield simultaneously when the system is under tension, which maximises the extent of the elastic range. The value of P_{opt} depends on the material and geometric properties of the tube and cable, and can be calculated from Eq. (1) [3], where A, E and f_y are as given in Table 1 and the subscripts c and t denote cable and tube, respectively. Connecting collars were employed at quarter points to ensure that the members did not buckle under the initial prestress [3]. From the measured properties, it was determined that P_{opt} = 189 kN for the S460 members and 167 kN for the S690 members. Note that the actual levels of prestress achieved in the experiments differed slightly from these target values and are reported in the following sections.

$$P_{opt} = \left(\frac{A_c A_t}{A_t E_t + A_c E_c} \right) \left(f_{cy} E_t - f_{ty} E_c \right) \text{, but } P_{opt} \le f_{ty} A_t \text{ and } f_{cy} A_c \qquad (1)$$

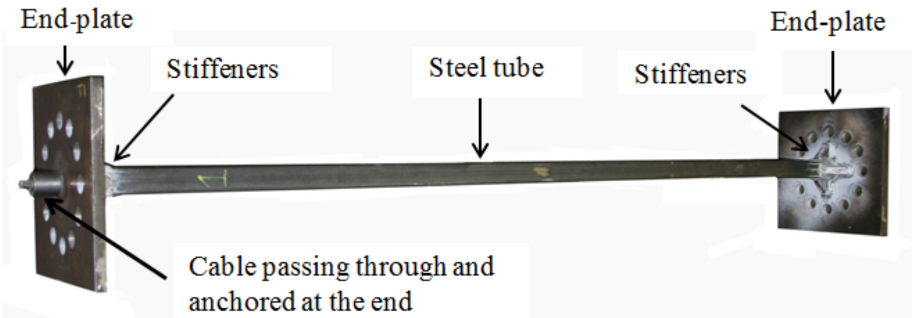

Fig. 1: Configuration of the cable-in-tube specimens

Table 1: Measured material and geometric properties of steel tubes and cable

Component	E (N/mm^2)	f_y (N/mm^2)	A (mm^2)
S460 SHS 50×50×5	210000	505	858
S690 SHS 50×50×5	208000	759	841
Cable	130000	1703	151

2.2 Tensile member tests and results

A total of 12 members were tested under tensile loading. The measured dimensions and prestress levels of the tensile specimens are presented in Table 2, where L_0, h, b, t and r_{ex} are the initial member length before prestressing, depth, width, wall thickness and average outer corner radius of the tube members, respectively, and P_i is the actual initial prestress level achieved. An Intron 2000kN machine was employed for the tensile member tests. The end-plates of the specimens were bolted onto the base and moving head of the machine, and displacement control was used to load the specimens at a rate of 0.5 mm/min. The applied load, axial displacement and four longitudinal strains at the mid-height of the tubes were recorded during the tests at 1 s intervals. The obtained axial load-displacement curves are plotted in Figs 3(a) and 3(b) for the S460 and S690 specimens, respectively. The results are discussed in Section 4.

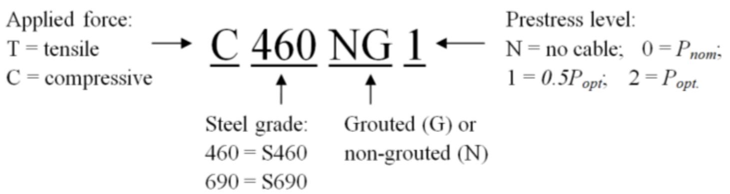

Fig. 2: Labelling convention for cable-in-tube test specimens

Table 2: Measured geometric dimensions and prestress levels of tensile members

Specimen	L_0 (mm)	h (mm)	b (mm)	t (mm)	r_{ex} (mm)	P_i (kN)
T460NGN	1954	50.07	50.36	5.01	5.63	N/A
T460NG0	1997	50.27	50.35	5.01	5.63	4.7 (P_{nom})
T460NG1	2001	50.28	49.96	5.01	5.63	77.3 ($0.41P_{opt}$)
T460NG2	2000	50.32	50.15	5.01	5.63	153.7 ($0.81P_{opt}$)
T460G1	2002	50.11	50.25	5.01	5.63	84 ($0.44P_{opt}$)
T460G2	2001	50.14	49.88	5.01	5.63	150.7 ($0.80P_{opt}$)
T690NGN	2000	50.18	50.43	4.91	5.88	N/A
T690NG0	2000	50.27	50.37	4.91	5.88	5.7 (P_{nom})
T690NG1	1999	50.11	50.36	4.91	5.88	60.5 ($0.36P_{opt}$)
T690NG2	2003	50.50	50.12	4.91	5.88	131.0 ($0.78P_{opt}$)
T690G1	2001	50.26	50.40	4.91	5.88	86.2 ($0.52P_{opt}$)
T690G2	1954	50.38	50.28	4.91	5.88	124.3 ($0.74P_{opt}$)

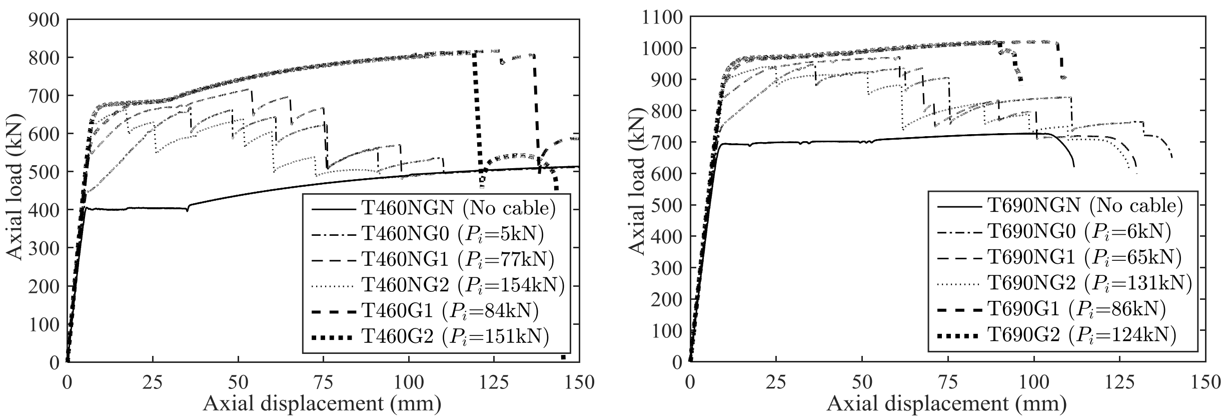

a) S460 members b) S690 members

Fig. 3: Axial load vs displacement relationship of tensile members

2.2 Compressive member tests and results

The dimensions and prestress levels of the compressive specimens are reported in Table 3, where ω_i is the measured initial bow imperfection amplitude derived from strain gauge readings [5]. Fig. 4 illustrates the test setup. Pin-ended boundary conditions were applied through hardened steel knife edge supports, which allow only in-plane rotation of the members about one axis. Cylinders were used to connect the knife edges to the end-plates, encasing the anchoring system at both ends. The distance between the top and bottom knife edges was taken as the buckling length L_{cr} of the specimens. The monitored variables during testing included all those in the tensile member tests plus the lateral deflection at mid-height, which was recorded using a string pot. The load-lateral deflection curves for the S460 and S690 specimens are shown in Figs 5(a) and 5(b), respectively.

Table 3: Measured dimensions and prestress levels of compressive members

Specimen	L_0 (mm)	h (mm)	b (mm)	t (mm)	r_{ex} (mm)	ω_i (mm)	P_i (kN)
C460NG0	1003	50.32	50.19	5.01	5.63	1.28	6.8 (P_{nom})
C460NG2	1002	50.11	50.31	5.01	5.63	1.58	125.6 ($0.67P_{opt}$)
C460G0	1001	50.13	50.42	5.01	5.63	0.92	7.1 (P_{nom})
C460G1	1002	50.36	50.10	5.01	5.63	1.61	70.8 ($0.37P_{opt}$)
C460G2	1002	50.11	50.40	5.01	5.63	1.03	152.7 ($0.81P_{opt}$)
C690NG0	1000	50.42	50.14	4.91	5.88	0.82	3.7 (P_{nom})
C690NG2	1000	50.38	50.20	4.91	5.88	0.81	120.8 ($0.72P_{opt}$)
C690G0	1000	50.11	50.35	4.91	5.88	0.44	5.0 (P_{nom})
C690G1	1002	50.14	50.39	4.91	5.88	1.88	65.2 ($0.39P_{opt}$)
C690G2	1001	50.26	50.26	4.91	5.88	0.06	123.5 ($0.74P_{opt}$)

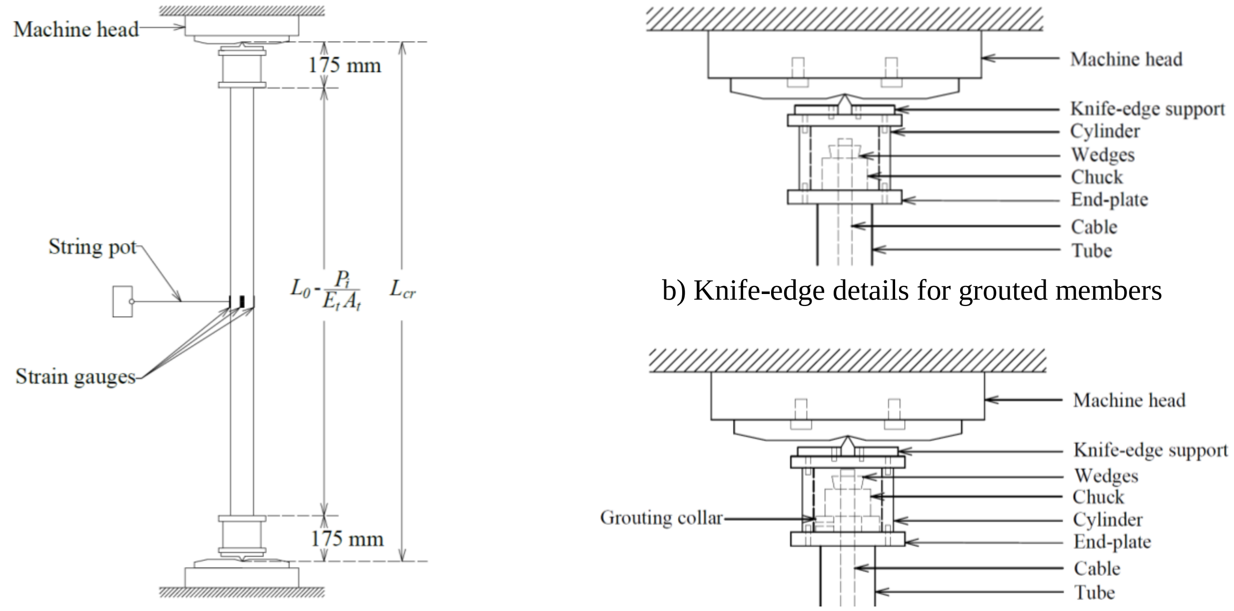

a) Schematic setup

b) Knife-edge details for grouted members

c) Knife-edge details for non-grouted members

Fig. 4: Compressive test setup

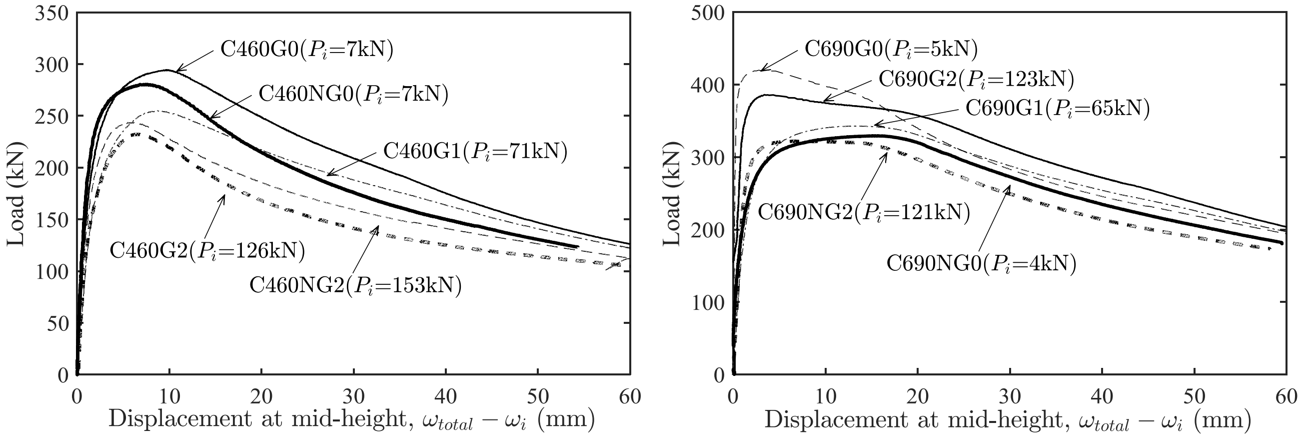

a) S460 members

b) S690 members

Fig. 5: Load-lateral deflection curves compressive members

3. FE validation and parametric study

Numerical modelling was conducted initially to replicate the experimental results and subsequently to generate parametric results for prestressed elements of different geometries. Only compressive members were examined in the numerical study since the tensile behaviour of the members could be accurately captured through simple analytical models.

3.1 Modelling assumptions

The components of the numerical models were the SHS tube, prestressing cable, connecting collars and confined grout for the grouted specimens. A fine mesh of three-dimensional eight node (C3D8) solid elements was used to model all the components. The mesh size reported in [6] was adopted herein. The measured material properties of the cables and steel tubes were employed in the models. The material model of the grout was derived based on the grout cube strength, following the approach described in [6]. A friction coefficient of 0.25 was used to define the tangential behaviour of the contact faces of the tube–grout and grout–cable interface elements. An initial imperfection in the form of the first eigenmode with the amplitude reported in Table 3 was assigned to the models. In the nonlinear analysis, the prestressing was achieved by assigning initial stresses to the elements of each component. The loaded models were in compression via displacement control.

3.2 FE validation and parametric study

The FE models were able to capture accurately the observed the load–deformation history of the prestressed members under compression. This is shown in Fig. 6, in which the results of the C460NG0 and C460G0 models are given as examples. Based upon the validated numerical models, an extensive parametric study was conducted for the development and assessment of design proposals. A total of 192 FE models, comprising 8 member slenderness values (0.5-2.25), 2 cable sizes (A_c =100 or 150 mm^2), 3 prestress levels (P_{nom}, 0.5P_{opt} and P_{opt}), 2 grout conditions (grouted and non-grouted) and 2 steel grades (S460 and S690), were simulated. An initial imperfection of L/1000 was applied to all models.

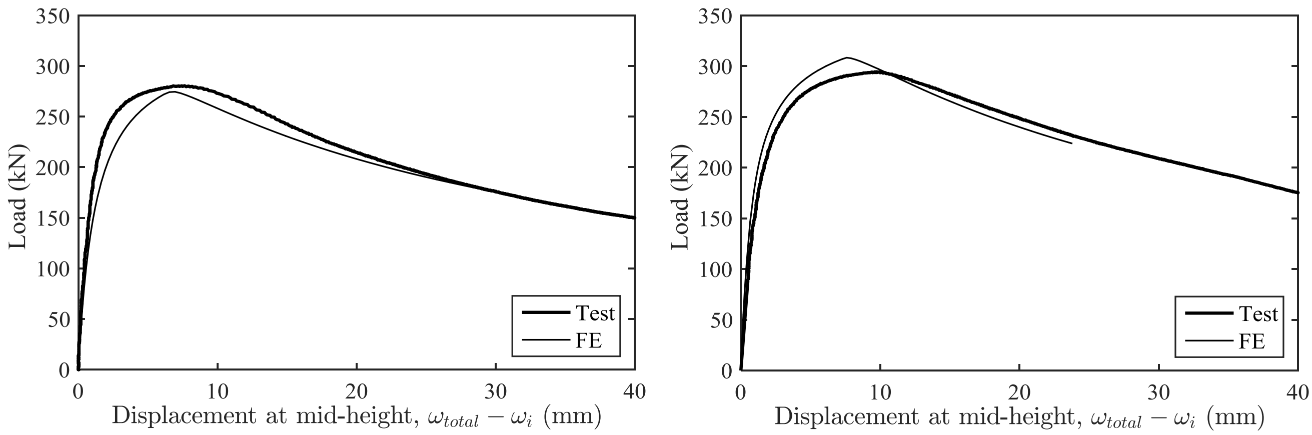

a) C460NG0 b) C460G0

Fig. 6: Validation of FE models for compressive specimens

4. Analysis of results and design recommendations

4.1 Tensile members

The tensile response of the prestressed members could be predicted analytically. By combining the measured geometries (i.e. section sizes and member length) with assumed bi-linear stress-strain material models of the cables and steel tubes, analytical axial load-displacement relationships can be derived [3]. Figs 7(a) and 7(b) demonstrate that the analytical results match closely the test results of the non-grouted members. The T460NGN and T690NGN results have also been included in Figs 7(a) and 7(b) for comparison purposes.

From Figs 7(a) and 7(b), it is clear that the introduction of prestressing cables can significantly improve the strength of the cable-in-tube systems. Furthermore, the addition of prestress can be seen to extend the elastic response of the cable-in-tube system. The presence of the grout had a minimal effect on the strength of the system, but was found to improve the ductility.

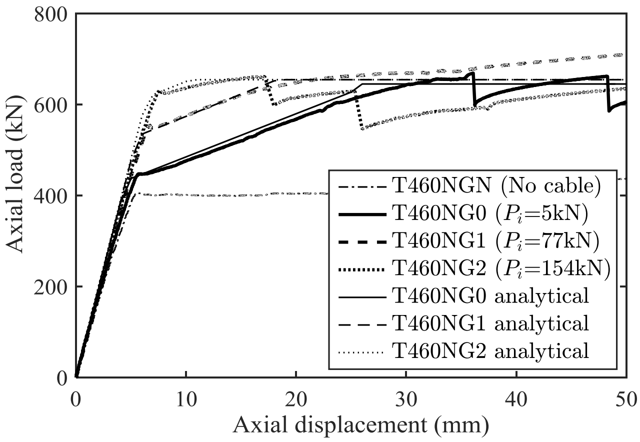

a) S460 non-grouted tensile members

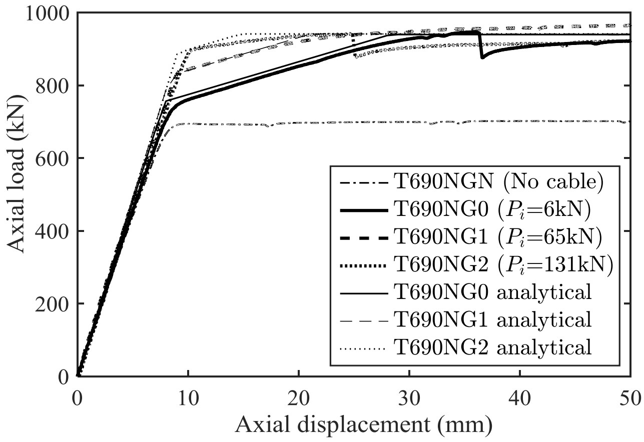

b) S690 non-grouted tensile members

Fig. 7: Analytical and test results of non-grouted tensile members

4.2 Compressive members

Prestressing is detrimental for self-anchored cable-in-tube systems in compression. However, the observed reduction in resistance was not as large as the applied initial prestress. This is illustrated in Figs 5(a) and 5(b), where the C460NG2 (P_i = 126kN) had only a 70kN resistance reduction in comparison with the C460NG0 member, and the capacity of the C690NG2 specimen (P_i = 121kN) was almost the same as the C690NG0 specimen. This is due to the absence of second order bending moments induced by prestressing: i.e. the prestress force remains aligned with the centroidal axis of the member, even in the deformed configuration. The presence of grout was shown, as expected, to increase the compressive capacity - see Figs 5(a) and 5(b).

The design of cable-in-tube systems under compression has been studied in Gosaye et al. [4], where a method based on the Perry-Robertson approach [7] for conventional column design was developed, and termed the modified Perry-Roberston approach. The method employs the same framework as Eurocode 3 [8] for column design, but accounts for the prestressing cables and grout, as expressed in Eqs (2)-(7), where the symbols are consistent with those used in Eurocode 3 [8]. The compressive capacity of the system is expressed as the plastic resistance of the cross-section multiplied by a reduction factor to account for member instability,

$$N_{u,cal} = \chi_p N_{pl} \tag{2}$$

where N_{pl} is defined in Eq. (3) for non-grouted and grouted members (denoted with g),

$$N_{pl} = A_t f_{ty};\ N_{pl,g} = A_t f_{ty} + A_g f_{gk} \tag{3}$$

and χ_p is related to the member slenderness through Eqs (4) and (5).

$$\chi_p = \frac{(1 - P_i / N_{pl})}{\alpha_k \left[\phi_p - \sqrt{\phi_p^2 - \dfrac{(1 - P_i / N_{pl})}{\alpha_k} \bar{\lambda}^2} \right]} \tag{4}$$

$$\phi_p = \frac{(1 - P_i / N_{pl}) \bar{\lambda}^2 + \left[\alpha_k + \alpha(\bar{\lambda} - 0.2) \right]}{2\alpha_k} \tag{5}$$

$\bar{\lambda}$ and α_k are defined in Eqs (6) and (7), respectively, for members without and with grout, where α is the imperfection factor, with a value of 0.13, corresponding to buckling curve a_0 as recommended by EC3 [8] for S460 and S690 hot-finished tubular members.

$$\bar{\lambda} = \sqrt{\frac{N_{pl}}{N_{cr}}};\quad \bar{\lambda}_g = \frac{L_{cr}}{\pi} \sqrt{\frac{N_{pl}}{E_t I_t + 0.6 E_{gm} I_g}} \tag{6}$$

$$\alpha_k = \frac{K_t}{K_c + K_t};\ \alpha_{k,g} = \frac{K_t + K_g}{K_c + K_t + K_g} \tag{7}$$

In Eq. (7), K_c, K_t and K_g are the axial stiffness of the cable, tube and grout (A_cE_c/L, A_tE_t/L and A_gE_{gm}/L), respectively. Note that for the case of very small initial prestress (i.e. $P_i < N_{b,t}K_c/(K_c+K_t)$ for non-grouted members and $P_i < N_{b,t}K_c/(K_c+K_t+K_g)$ for grouted members, where $N_{b,t}$ is the buckling resistance of the steel tube), the cable will slacken before the member fails, hence the design is equivalent to the case without prestressing, which leads to $P_i = 0$ and $\alpha_k = 1$in Eqs (4) and (5).

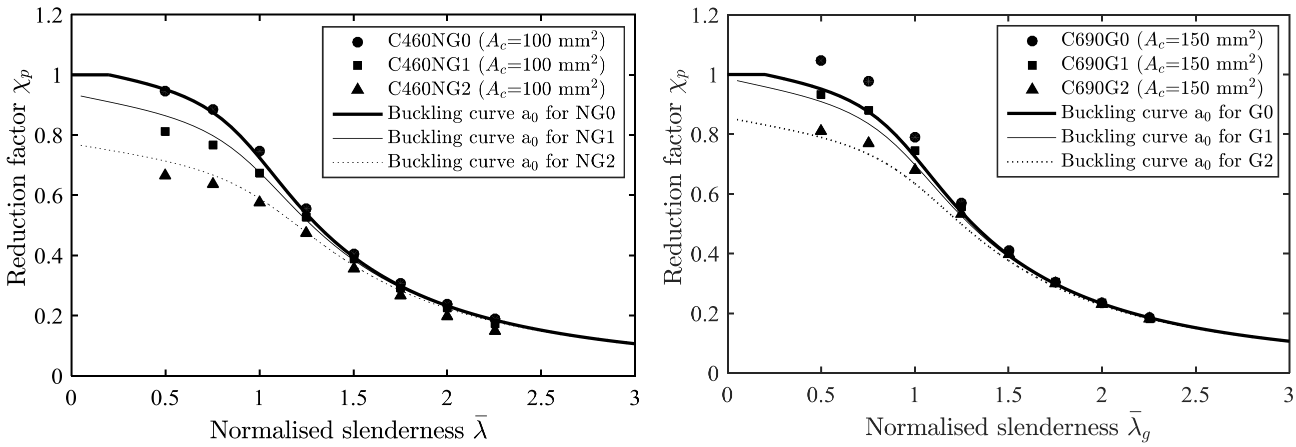

a) C460NG (A_c=100 mm^2) b) C690G (A_c=150 mm^2)

Fig. 8: Assessment of the modified Perry-Robertson approach

The C460NG (A_c=100 mm^2) and C690G (A_c=150 mm^2) FE results are plotted in Figs 8(a) and 8(b), respectively, to assess the design curves determined from the modified Perry-Robertson approach [4]. In general, this approach can provide a good estimation of the compressive resistance of cable-in-tube systems. However, buckling curve a_0 slightly overestimates the strength of the S460 0.5P_{opt} and P_{opt} models, as shown in Fig. 8(a). It also underestimates the S690 results for the complete range of prestress levels considered, especially for the stocky members, as demonstrated in Fig. 8(b). Alternative buckling curves may therefore need to be considered for prestressed HSS tubes.

5. Conclusions

The tensile and compressive behaviour of cable-in-tube systems has been examined through a series of experimental and numerical investigations. Tensile resistance was shown to be enhanced by the addition of the cable while the application of prestress was needed to extend the elastic range and hence the overall performance of the cable-in- tube system. Prestressing was found to reduce the compressive resistance of the system, but the reduction in strength was shown to be much less than the applied prestress due to the absence of second order bending moments. FE models, validated against the experiments, were employed in order to generate parametric results for the assessment of a modified Perry-Robertson design method [4]. Buckling curve a_0 adopted in EC3 [8] was shown to yield some unsafe predictions for the S460 $0.5P_{opt}$ and P_{opt} members, but was safely applicable to the S690 members.

Acknowledgments

The research has received funding from the Research Fund for Coal and Steel (RFCS) under grant agreement No. RFSR CT 2012-00028. V&M DEUTSCHLAND GMBH is acknowledged for the supply of the test specimens. The authors are indebted to Mr Gordon Herbert, Mr Paras Shah and Mr Stephen Okeghie for their assistance during the tests.

References

[1] Li H, Schmidt L. "Post-tensioned and shaped hypar space trusses", *Journal of Structural Engineering, ASCE 1997*, 123(2), 130-137, 1997.
[2] Schmidt L C, Li H. "Studies on post-tensioned and shaped space-truss domes", *Structural Engineering and Mechanics*, 6, 693-710, 1998.
[3] Gosaye J, Gardner L, Wadee A, Ellen M. "Tensile performance of prestressed steel elements", *Engineering Structures*, 79, 234-243, 2014.
[4] Gosaye J, Gardner L, Wadee A, Ellen M. "Compressive behaviour and design of prestressed steel elements", *Structures*, 5, 76-87, 2016.
[5] Zhao O, Rossi B, Gardner L, Young B. "Behaviour of structural stainless cross-sections under combined loading – Part I: Experimental study", *Engineering Structures*, 89, 236-246, 2014.
[6] Tao Z, Wang Z, Yu Q. "Finite element modelling of concrete-filled steel stub columns under axial compression", *Journal of Constructional Steel Research*, 89, 121-131, 2013.
[7] Ayrton W E, Perry J. "On struts", *The Engineer (London)*, 62, 464-465, 1886.
[8] EN 1993-1-1:2005. "Eurocode 3: Design of steel structures – part 1-1: General rules and rules for buildings", *Brussels: European committee for standardization (CEN)*, 2005.